

Recently, a novel strategy utilizing activatable photosensitizers has been posited.^{8,13–17} In these systems the excited states of the porphyrinic chromophore are quenched via electron- or energy-transfer processes, and can be regained in the presence of certain enzymes or by preferential localization. We have previously reported the synthesis of two different activatable systems based upon aggregation induced quenching. In the first example, a polymeric nanoparticle was prepared in which the potent photosensitizer, *meso*-tetraphenylporpholactol, was rendered nonphototoxic upon encapsulation.¹³ When incubated with lipid or cells, the photosensitizer was released and regained its phototoxicity. In vivo, this preparation was able to eradicate cancer in an entire cohort of mice. In the second system, multiple chlorin *e*₆ chromophores were conjugated to a polylysine graft copolymer backbone which is readily cleaved by Cathepsin B, a tumor-associated protease.¹⁸ Upon conjugation, the dyes exhibited an 86% decrease in fluorescence, and an 80% decrease in singlet oxygen generation, which could be regained by incubation with the protease.

One other strategy that has been investigated is the conjugation of quencher molecules to the porphyrinic macrocycle via linker moieties that do not participate in the π -conjugation of the chromophore.^{14–17} A number of quenchers have been investigated, including metalloporphyrins, dye molecules, or antioxidants. In some of these systems, the quencher molecule is separated from the chromophore by an enzyme cleavable linker. This allows for the spatial control of photosensitizer activation, as the construct will remain essentially nonfluorescent and nonphototoxic until it reaches the site of interest and is activated. These systems are highly useful in the treatment of diseases in which specific enzymes are upregulated, as compared to their expression in healthy tissues.

Analogous to the development of activatable photosensitizers, much research has been accomplished with regard to the development of activatable fluorescent probes, from which novel techniques can be learned and applied to porphyrinic systems. A number of groups have described the synthesis of fluorescent probes that are activated by thiols.^{19–21} The potential utility of these agents is that thiols represent a class of molecules responsible for the maintenance of cellular redox homeostasis, which may be altered in cases of disease or infection. In particular, the relative levels of thiols such as glutathione, cysteine, and homocysteine and their oxidized disulfide forms have been implicated in the

development of specific diseases, including Alzheimer's, cancer, and cardiovascular disease.^{22–25} In their construct, the authors utilized a classic donor- π -acceptor architecture based upon the formation of a thiol-cleavable arenesulfonamide. The resulting probe exhibited superb stability in the presence of oxygen or nitrogen nucleophiles, yet was readily cleaved by thiols, such as cysteine, glutathione, and dithiothreitol. This probe demonstrated a 120-fold increase in fluorescence upon activation, and serves as a potential model for activatable photosensitizers.

Herein, we report a novel paradigm for excited state quenching based upon the conjugation of 2,4-dinitrobenzene (DNB) to the periphery of *meso*-tetraphenylporphyrins via thiol-labile sulfonamide linkages. These model systems, derived from mono-, di-, tri-, and tetra(*p*-aminophenyl)porphyrin have been synthesized and their photophysical properties have been investigated. In addition, methods to further functionalize the amines with moieties that allow for the modulation of the polarity of the porphyrin or conjugation to biomolecules or nanoparticles have been developed. These photosensitizer systems, while imparting specificity for thiol-containing analytes, serve as a template on which to base future substrate-specific agents.

Results and Discussion

Synthesis and characterization of sulfonamidophenylporphyrins (SPP). *meso-p*-Aminophenylporphyrins bearing 1 through 4 anilines have previously been reported for use in a number of applications.²⁶ These macrocycles can be synthesized using a variety of methodologies. For mono-, di-, and tri(*p*-aminophenyl)porphyrins (**1**, **2c**, **2t**, and **3**, respectively, Scheme 1), the most facile synthesis involved the nitration of *meso*-tetraphenylporphyrin (TPP) with NaNO₂, followed by reduction with SnCl₂·2H₂O.²⁶ The four derivatives including the *cis*- and *trans*-isomers of **2** (**2c** and **2t**) were readily synthesized by adding varying ratios of NaNO₂ to a TFA solution of TPP. While it would have been optimal to utilize the same strategy to synthesize the tetra(*p*-aminophenyl)porphyrin derivative (**4**), it is exceedingly difficult to add more than three nitro-substituents to the *meso*-phenyl groups.²⁶ Instead, the *meso*-tetra(*p*-aminophenyl)porphyrin was synthesized by the condensation of *p*-nitrobenzaldehyde with pyrrole in refluxing propionic acid, followed by SnCl₂·2H₂O reduction of the nitro groups to the corresponding amines.³¹

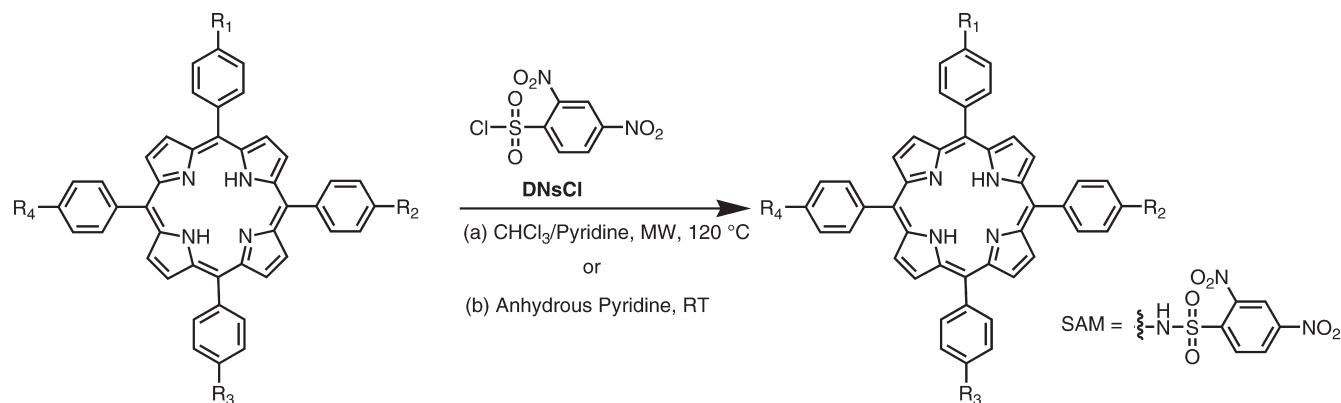
The mono- and disulfonamidophenylporphyrins (SPP, **1SAM**, **2cSAM**, and **2tSAM**, respectively, Scheme 1) were synthesized via microwave-assisted syntheses. The advantage of this method is that it allows for relatively short reaction times with moderate to good yields.^{14,27} Dissolution of **1**, **2c**, or **2t** and excess 2,4-dinitrobenzenesulfonyl chloride (DNsCl) in a mixture of CHCl₃/pyridine followed by microwave irradiation gave the mono-SPP **1SAM** in 70% yield, the *cis*-di-SPP **2cSAM** in 57% yield, and the *trans*-di-SPP **2tSAM** in 81% yield.

Our initial attempts to synthesize the tri-SPP derivative (**3SAM**) via the microwave-mediated procedure described

- (14) McCarthy, J. R.; Weissleder, R. *ChemMedChem* **2007**, *2*, 360–365.
 (15) Stefflova, K.; Chen, J.; Zheng, G. *Curr Med Chem* **2007**, *14*, 2110–2125.
 (16) Stefflova, K.; Li, H.; Chen, J.; Zheng, G. *Bioconjug Chem* **2007**, *18*, 379–388.
 (17) Zheng, G.; Chen, J.; Stefflova, K.; Jarvi, M.; Li, H.; Wilson, B. C. *Proc. Natl. Acad. Sci. U. S. A.* **2007**, *104*, 8989–8994.
 (18) Choi, Y.; Weissleder, R.; Tung, C. H. *Cancer Res.* **2006**, *66*, 7225–7229.
 (19) Bouffard, J.; Kim, Y.; Swager, T. M.; Weissleder, R.; Hilderbrand, S. A. *Org. Lett.* **2008**, *10*, 37–40.
 (20) Jiang, W.; Fu, Q.; Fan, H.; Ho, J.; Wang, W. *Angew. Chem., Int. Ed. Engl.* **2007**, *46*, 8445–8448.
 (21) Shibata, A.; Furukawa, K.; Abe, H.; Tsuneda, S.; Ito, Y. *Bioorg. Med. Chem. Lett.* **2008**, *18*, 2246–2249.
 (22) Heafield, M. T.; Fearn, S.; Steventon, G. B.; Waring, R. H.; Williams, A. C.; Sturman, S. G. *Neurosci. Lett.* **1990**, *110*, 216–220.
 (23) Nekrassova, O.; Lawrence, N. S.; Compton, R. G. *Talanta* **2003**, *60*, 1085–1095.
 (24) Nygard, O.; Nordrehaug, J. E.; Refsum, H.; Ueland, P. M.; Farstad, M.; Vollset, S. E. *N Engl J Med* **1997**, *337*, 230–236.

- (25) Refsum, H.; Ueland, P. M.; Nygard, O.; Vollset, S. E. *Annu Rev Med* **1998**, *49*, 31–62.
 (26) Luguza, R.; Jaquinod, L.; Fronczek, F. R.; Vicente, M. G. H.; Smith, K. M. *Tetrahedron* **2004**, *60*, 2757–2763.
 (27) Dean, M. L.; Schmink, J. R.; Leadbeater, N. E.; Bruckner, C. *Dalton Trans* **2008**, 1341–1345.

SCHEME 1. Synthesis of Aromatic SPP



- 1**, $\text{R}_1 = \text{NH}_2$, $\text{R}_2 = \text{R}_3 = \text{R}_4 = \text{H}$
2c, $\text{R}_1 = \text{R}_2 = \text{NH}_2$, $\text{R}_3 = \text{R}_4 = \text{H}$
2t, $\text{R}_1 = \text{R}_3 = \text{NH}_2$, $\text{R}_2 = \text{R}_4 = \text{H}$
3, $\text{R}_1 = \text{R}_2 = \text{R}_3 = \text{NH}_2$, $\text{R}_4 = \text{H}$
4, $\text{R}_1 = \text{R}_2 = \text{R}_3 = \text{R}_4 = \text{NH}_2$

- method (a), **1SAM**, $\text{R}_1 = \text{SAM}$, $\text{R}_2 = \text{R}_3 = \text{R}_4 = \text{H}$, 70%
 method (a), **2cSAM**, $\text{R}_1 = \text{R}_2 = \text{SAM}$, $\text{R}_3 = \text{R}_4 = \text{H}$, 57%
 method (a), **2tSAM**, $\text{R}_1 = \text{R}_3 = \text{SAM}$, $\text{R}_2 = \text{R}_4 = \text{H}$, 81%
 method (b), **3SAM**, $\text{R}_1 = \text{R}_2 = \text{R}_3 = \text{SAM}$, $\text{R}_4 = \text{H}$, 78%
 method (b), **4SAM**, $\text{R}_1 = \text{R}_2 = \text{R}_3 = \text{R}_4 = \text{SAM}$, 50%

above failed due to solubility issues associated with the use of a large excess DNsCl, as 8 equivalents per amine were utilized and the reaction is limited to a small reaction volume (8 mL). Hence, a milder, room temperature method was utilized. A solution of porphyrin **3** in anhydrous pyridine was treated with DNsCl (10 equiv) and allowed to stir 22 h, at which time the resulting crude mixture was purified by column chromatography affording the desired tri-SPP (**3SAM**) in 78% yield (Scheme 1). The tetra-SPP derivative, **4SAM**, was synthesized by the same procedure, and resulted in a 50% isolated yield.

The presence of the sulfonamide substituents in the products was confirmed by ^1H NMR spectroscopy. In all cases, the spectra showed a characteristic singlet corresponding to the sulfonamide protons at approximately 11.5 ppm, with additional signals in the aromatic region for the protons of the dinitrobenzene. In addition, a peak at ~ -2 ppm was

observed, which is typically associated with the two pyrrolic amine protons in the core of the free base porphyrin. While the *cis*- and *trans*- isomers of the di-SPP were synthesized from the respective purified aminophenylporphyrin derivatives,²⁶ the products can be readily distinguished by looking at the symmetry of their respective spectra (see Figure S1). Both products, **2cSAM** and **2tSAM**, possess C_2 symmetry, yet have different axes of symmetry. For the *cis* isomer, **2cSAM**, the symmetry axis bisects the pyrrolic β protons, which results in the appearance of two singlets for four of the eight β protons. In the *trans* isomer, on the other hand, the symmetry axis is through the *meso*-phenyl position, resulting in four sets of doublets for the β protons. The tri- and tetrasulfonamide derivatives, **3SAM** and **4SAM**, were rather unremarkable aside from their C_2 and C_4 symmetries, respectively.

The UV-vis absorption spectra of the aminophenylporphyrins (Figure 1A) demonstrated decreasing extinction

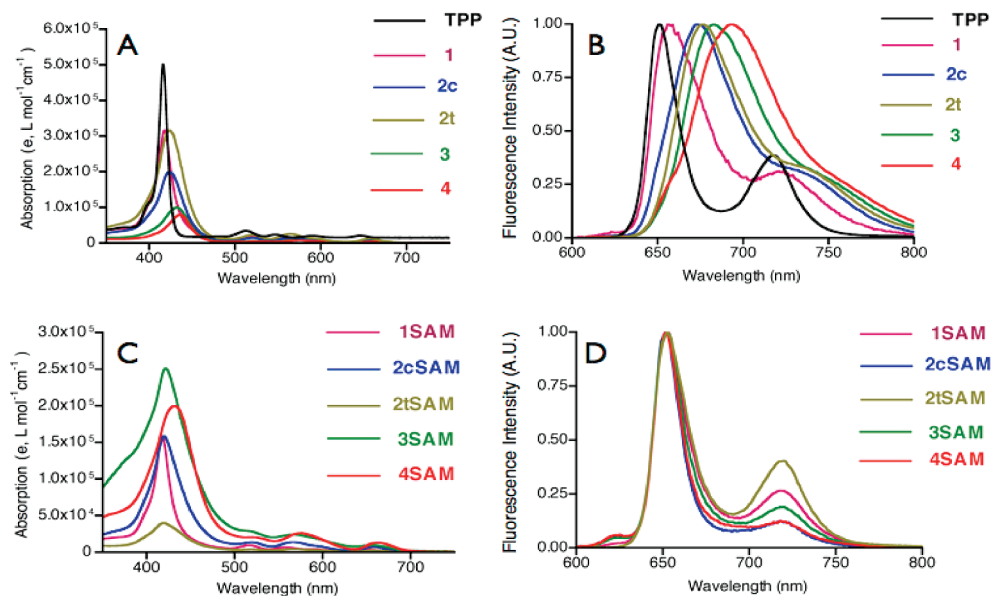


FIGURE 1. Absorption spectra of (A) aminophenyl and (C) sulfonamidophenyl porphyrins. Normalized emission spectra of (B) aminophenyl and (D) sulfonamidophenyl porphyrins excited at the respective Soret band maxima. (See Table 1 for values. All spectra acquired in DMF.)

TABLE 1. Photophysical Properties of Synthesized Porphyrins^a

compd	Soret (nm)	log ϵ (L mol ⁻¹ cm ⁻¹)	fluorescence emission (nm)	Φ_{FI}	Φ_{Δ}
TPP	417	5.7	651	0.15	0.64
1	418	5.5	664	0.05	0.22
2c	424	5.3	674	0.13	0.37
2t	424	5.5	674	0.14	0.42
3	432	5	682	0.24	0.47
4	434	4.9	693	0.24	0.53
1SAM	418	5.2	653	0.02	0.11
2cSAM	420	5.2	652	0.01	0.01
2tSAM	421	4.6	652	0	0.01
3SAM	422	5.4	651	0.01	0.05
4SAM	440	5.3	653	0.00	0.01
7	424	4.9	660	0.17	0.57
8	422	5.1	656	0.08	0.23
1SAM-TE	417	5.5	651	0.05	0.16
1SAM-AA	418	5.5	651	0.03	0.23
1SAM-PS	418	5.2	650	0.05	0.23
1SAM-mPEG	417	4.5	650	0.05	0.19
4SAM-mPEG	420	5.1	651	0.02	0.07
4-mPEG	437	5.3	686	0.3	0.61

^aAll data were collected in DMF at room temperature.

coefficients with increasing number of amine substituents in DMF (Table 1). This is likely due to the formation of aggregates, which are not observed when the porphyrins are dissolved in THF (Table S1). Concomitant with this decrease in extinction coefficient is a bathochromic shift of the absorption spectrum. This translates into red-shifted fluorescence emission spectra, with shifts up to 17 nm as compared to **TPP** (Figure 1B). Interestingly, the fluorescence quantum yields of the aminophenylporphyrins increase with increasing amination. Previous reports have described enhanced emission properties resulting from the aggregation of the porphyrinic dyes,²⁸ and we believe that this may be the origin of these observations.

Upon sulfonamide formation, the Soret bands of the porphyrins return to approximately the same wavelength as **TPP** (Figure 1C) with equivalent extinction coefficients (Table 1). The contribution of the DNB to the absorption spectrum is seen in the shape of the Q bands, as well as a broadened Soret band. The only product that does not follow this pattern is the tetrasulfonamide **4SAM**, which is bathochromically shifted with a severely broadened Soret band due to decreased solubility in DMF and aggregation. In all cases, the porphyrins exhibited excited state quenching, with negligible fluorescence emission or singlet oxygen generation.

Synthesis and characterization of sulfonamidophenylporphyrin variants. While the above preparations involve the conjugation of the sulfonamide directly to the *meso*-phenyl groups, we also wanted to examine whether excited state quenching would still be observed if the DNB sulfonamides were separated from the porphyrin core by short aliphatic linkers. In order to achieve this, a solution of triaminophenylporphyrin porphyrin **3** in CHCl₃/pyridine was treated with N,N'-dicyclohexylcarbodiimide (DCC) and N-Fmoc-amido-dPEG₂-acid **5**, followed by microwave irradiation. After workup, the Fmoc protecting group was removed by stirring intermediate **6** in DMF/piperidine at room temperature for 3 h. The resulting crude reaction mixture was purified by HPLC to afford the PEG-amine porphyrin derivative

7 in 73% yield (Scheme 2). The corresponding sulfonamide derivative was synthesized by dissolution of **7** in DMF/TEA followed by the treatment with excess DNsCl. The reaction mixture was stirred at room temperature for 2 days under an argon atmosphere, and then purified by preparative HPLC affording the SPP derivative **8**. The triaminophenylporphyrin **3** was chosen for this synthesis because of its high yield from **TPP**, as well as the almost complete quenching of the excited states when converted to **3SAM**. As compared to the PEG-amine derivative **7**, the fluorescence and singlet oxygen quantum yields of SPP **8** decreased by 50% (Table 1). This decrease was far less than what was demonstrated in **3SAM** ($\Phi_{\text{FI}} = 0.01$, $\Phi_{\Delta} = 0.05$), thereby illustrating that the removal of the DNB moieties from the porphyrin core has a detrimental effect on their quenching potential.

Since the quenching efficiency of **8** was less than ideal, we decided to develop chemistries that would allow for the modulation of the polarity of the SPP or allow them to have reactive handles for conjugation to biomolecules or nanoparticles for in vitro or in vivo delivery. In order to do this, **1SAM** was utilized as a model compound, and was modified by alkylation of the sulfonamide to generate a tertiary amine.

Alkylation can be effected by reacting an alkyl bromide with the SPP in dry acetone with freshly powdered anhydrous K₂CO₃. In order to incorporate a carboxylic acid functionality, **1SAM** was reacted with *tert*-butyl bromoacetate. Upon complete conversion to the desired product the reaction mixture was purified by column chromatography affording a tertiary SPP (**1SAM-TE**) in 75% yield (Scheme 3). The ester group in the sulfonamidophenyl porphyrin **1SAM-TE** was hydrolyzed by the treatment with CH₂Cl₂/TFA (4:1) at room temperature affording **1SAM-AA** in quantitative yield. The protected acid was utilized in this synthesis due to the fact that the reaction between bromoacetic acid and the porphyrin did not result in product formation. This may be attributed to the fact that bromoacetic acid has low solubility in the reaction mixture.

In order to modulate the polarity of the SPP, the addition of discrete PEG chains and alkyl sulfonates were investigated as model modifications. The PEG chain was appended to the

(28) Causgrove, T. P.; Cheng, P.; Brune, D. C.; Blankenship, R. E. *J. Phys. Chem.* **1993**, *97*, 5519–5524.

SCHEME 4. Synthesis of Tertiary Sulfonamidophenyl Porphyrins Based on 4SAM

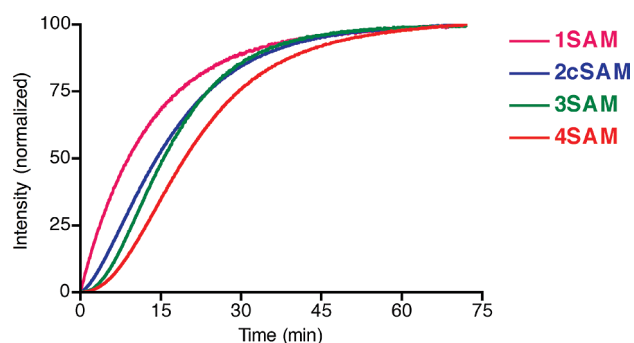
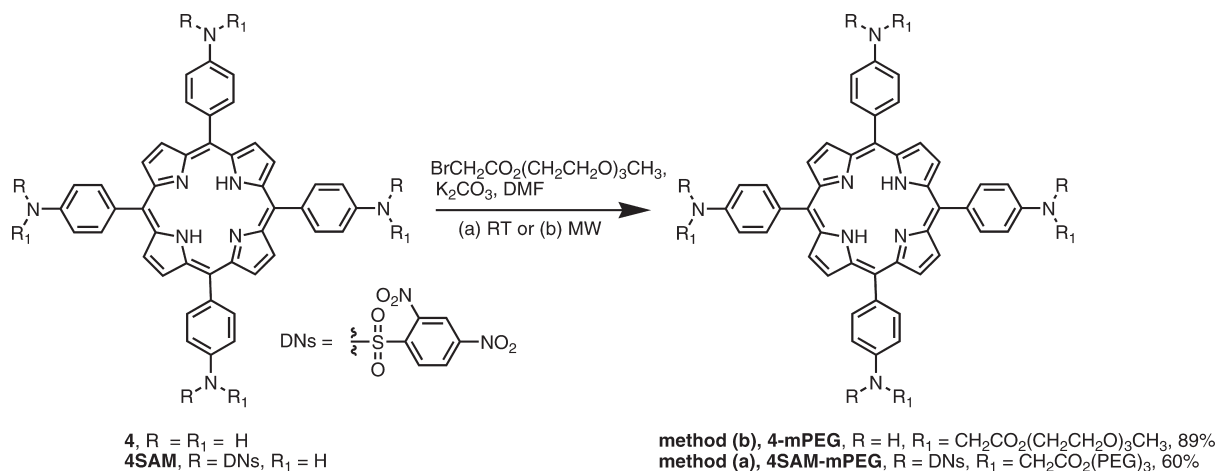


FIGURE 2. Relative rate of thioglycolic acid mediated cleavage of aromatic sulfonamidophenyl porphyrins in DMF.

PEG₃-bromoacetate at room temperature for 7 h to afford 4SAM-mPEG in 60% yield (Scheme 4). This derivative demonstrated a high degree of excited state quenching ($\Phi_{FI} = 0.02$, $\Phi_{\Delta} = 0.07$), as compared to its nonquenched analog 4-mPEG ($\Phi_{FI} = 0.3$, $\Phi_{\Delta} = 0.61$).

Profiling of excited state activation. The activation of the synthesized SPP derivatives were investigated, as the ultimate utility of the quenched photosensitizers relies upon the recovery of excited state processes. Incubation of the SPP with thiols, specifically thioglycolic acid, resulted in cleavage of the sulfonamide bond, liberating the respective aminophenylporphyrin (Figure 2). In these reactions, a solution of the SPP (0.5 μ M) in DMF was treated with a large excess of thiol (2.5 mM), and the kinetics were examined by monitoring the fluorescence intensity increase over time at the excitation and emission maxima of each resulting aminophenylporphyrin. While 2.5 mM thiol may seem excessive, relevant in vivo concentrations of thiols, such as glutathione, can be observed at millimolar concentrations.³⁰ As expected, the time required to effect complete excited state recovery increases with increasing number of arylsulfonamides. The shape of the resulting curves is also informative, with 1SAM displaying a hyperbolic shape characteristic of a pseudofirst order reaction. Since 2SAM, 3SAM, and 4SAM must each proceed through intermediates, which also display differing degrees of

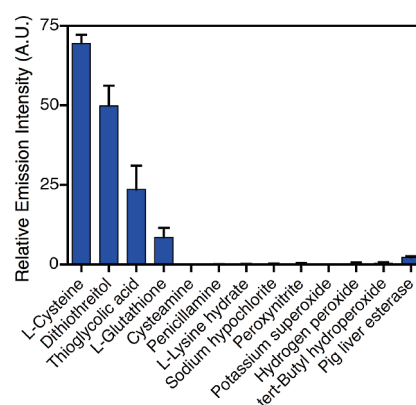


FIGURE 3. Response of tertiary sulfonamide 4SAM-mPEG to select analytes. Relative emission intensity of 0.5 μ M in DMF/HEPES (1:1, 2 mL, 10 mM, pH = 7.4) at 686 nm ($\lambda_{ex} = 437$ nm) after incubation at 37 °C for 15 min in the presence of 0.5 mM (final concentration) analyte. Pig liver esterase was utilized at a concentration of 2 units/mL.

quenching, and altered absorption and emission spectra, the line shape deviates from what is observed for 1SAM.

In order to examine the specificity of the sulfonamide cleavage reaction, the activation of the tertiary SPP, 4SAM-mPEG, was investigated with a number of potential substrates, including thiols (thioglycolic acid [TGA], L-cysteine [Cys], dithiothreitol [DTT], L-glutathione [GSH], cysteamine, penicillamine), nonthiol amino acids (Lysine) and oxidants (H₂O₂, *tert*-butyl hydroperoxide, potassium superoxide and NaOCl, peroxyntirite). The porphyrin was also reacted with pig liver esterase, a hydrolytic enzyme. The solutions of sulfonamidophenyl porphyrin (1 μ M) in DMF and analytes (1 mM, 1000 equiv) in HEPES buffer (pH = 7.4) were incubated at 37 °C for 15 min in DMF/HEPES (1:1, 2 mL, pH = 7.4). Each solution of porphyrin 4SAM-mPEG was then excited at 437 nm while monitoring the fluorescence intensity 686 nm. As has been illustrated previously,^{19,21} incubation of the SPP with amino acids that do not bear a thiol group and oxidants do not result in cleavage of the sulfonamide bond (Figure 3). Conversely, L-cysteine, DTT, TGA, and GSH all result in activation, although to varying degrees. At physiological pH, L-cysteine and DTT both bear overall neutral charges, whereas GSH and TGA are

(30) Townsend, D. M.; Tew, K. D.; Tapiero, H. *Biomed Pharmacother* 2003, 57, 145–155.

essentially anionic, which allows us to intimate that the charge of the molecule may alter its ability to cleave the sulfonamide bond. This is further supported by the fact that cysteamine, which should be positively charged in the utilized buffer system, does not react at all. In addition to charge effects, the sulfonamide cleavage must also contend with steric constraints. As compared to TGA, GSH is much larger and bulkier, which diminishes its ability to interact with the sulfonamide, resulting in a lesser degree of activation. Similarly, penicillamine, which is structurally similar to cysteine, except for the inclusion of two methyl groups on the amino acid side chain, does not react at all. This is likely due to the steric bulk adjacent to the thiol. This apparent selectivity for small, anionic or neutral charged thiol-containing analytes may serve to further increase specificity for in vivo applications, as these molecules are not expected to interact with proteins or oxidized thiols.

Conclusions

We have thus demonstrated that the conjugation of dinitrobenzene to the porphyrin macrocycle via a thiol-cleavable sulfonamide bond resulted in chromophores exhibiting excited-state quenching. The polarity of these dyes can be modulated by the conversion of the sulfonamide to the tertiary amine via reaction with hydrophilic alkyl bromides. In addition, a conjugatable linker can be introduced by reaction with *tert*-butyl bromoacetate followed by hydrolytic cleavage of the *tert*-butyl ester. The SPP are readily cleaved by a number of biologically relevant thiols, including glutathione and cysteine, and as such may demonstrate utility in vivo. Although the compounds synthesized herein demonstrated a novel paradigm for excited state quenching of porphyrinic photosensitizers, other derivatives can be envisioned bearing moieties activated by oxidants or other stimuli and, as such, are the continuing focus of our research.

Experimental Section

General Procedure for the Microwave-Assisted Synthesis of 1SAM, 2cSAM, and 2tSAM. To a solution of porphyrin (~30 mg) in CHCl_3 /pyridine (2.5 mL, 9:1) was added 2,4-dinitrobenzenesulfonyl chloride (8 equiv per amine). The reaction mixture was subjected to microwave irradiation with the following settings: $T = 120^\circ\text{C}$, $t = 25$ min, power = 300 W, $P_{\text{max}} = \text{off}$. Upon completion, methanol (5 mL) was added to the reaction mixture, followed by the addition of CH_2Cl_2 (20 mL) and water (10 mL). The organic layer was separated, dried over anhydr MgSO_4 , filtered, and evaporated to dryness. The solid residue was purified as detailed below.

5-[4-*N*-(2,4-Dinitrobenzene)sulfonamidophenyl]-10,15,20-triphenylporphyrin (1SAM). The solid residue was purified by flash chromatography (silica, CH_2Cl_2), and all fractions containing the product were combined and evaporated to dryness to afford a dark purple solid (30 mg, 70%): UV/vis (DMF) λ_{max} (log ϵ) 418 (5.25), 516 (4.06), 558 (3.91), 650 (3.60) nm; λ_{em} (DMF) 652 nm; ^1H NMR (500 MHz, DMF- d_7) δ -2.77 (br s, 2H), 7.78 (d, $J = 8.0$ Hz, 2H), 7.89 (m, 9H), 8.30 (br m, 8H), 8.71 (d, $J = 9.0$ Hz, 1H), 8.90 (br m, 9H), 9.13 (s, 1H), 11.46 (s, 1H) ppm; ^{13}C NMR (125 MHz, DMF- d_7) δ 119.5, 120.0, 120.5, 120.6, 120.65, 120.67, 123.4, 127.2, 127.8, 129.4, 132.8, 135.6, 137.2, 141.9, 148.7, 150.8 ppm; ESI-MS obsd 860; HRMS (ESI+ of $[\text{MH}^+]$, CH_3CN)

m/z calcd for $\text{C}_{50}\text{H}_{33}\text{N}_7\text{O}_6\text{S}$ 860.2286, found 860.2300; HPLC $t_{\text{R}} = 18.6$ min (using a gradient of 60% to 0% of buffer A over 25 min).

5,10-Bis[4-*N*-(2,4-dinitrobenzene)sulfonamidophenyl]-15,20-diphenylporphyrin (2cSAM). The solid residue was chromatographed [silica, $\text{CH}_2\text{Cl}_2 \rightarrow \text{CH}_2\text{Cl}_2$ /methanol (49:1)], and all fractions containing the product were combined and evaporated to dryness to afford a purple solid 2cSAM.

Alternate Synthesis of 2cSAM. A sample of porphyrin 2c (26 mg, 0.04 mmol)²⁶ was dissolved in anhydrous pyridine (2 mL) followed by the treatment with 2,4-dinitrobenzenesulfonyl chloride (0.11 g, 0.41 mmol). The reaction mixture was subjected to stirring for 27 h at room temperature. Upon completion, 1 M HCl (5 mL) was added to the reaction mixture, followed by the addition of CH_2Cl_2 (25 mL). The organic layer was separated, dried over anhydr MgSO_4 , filtered, and evaporated to dryness. The solid residue was chromatographed [silica, $\text{CH}_2\text{Cl}_2 \rightarrow \text{CH}_2\text{Cl}_2$ /methanol (49:1)], and all fractions containing the product were combined and evaporated to dryness to afford a purple solid 2cSAM (25 mg, 57%): UV/vis (DMF) λ_{max} (log ϵ) 420 (5.18), 520 (4.18), 568 (4.20), 660 (3.88) nm; λ_{em} (DMF) 652 nm; ^1H NMR (500 MHz, DMF- d_7) δ -2.81 (brs, 2H), 7.77 (d, $J = 8.0$ Hz, 4H), 7.89 (d, $J = 7.0$ Hz, 6H), 8.29 (m, 8H), 8.71 (d, $J = 9.0$ Hz, 2H), 8.88 (m, 8H), 8.90 (d, $J = 2.0$ Hz, 2H), 9.12 (d, $J = 2.0$ Hz, 2H), 11.47 (s, 2H) ppm; ^{13}C NMR (125 MHz, DMF- d_7) δ 119.6, 120.5, 120.6, 120.7, 127.2, 132.8, 135.6, 137.2, 141.9, 148.7, 150.8 ppm; ESI-MS obsd 1105; HRMS (ESI+ of $[\text{MH}^+]$, CH_3CN) m/z calcd for $\text{C}_{56}\text{H}_{36}\text{N}_{10}\text{O}_{12}\text{S}_2$ 1105.2028, found 1105.2019; HPLC $t_{\text{R}} = 19.04$ min (using a gradient of 60% to 0% of buffer A over 25 min).

5,15-Bis-[4-*N*-(2,4-dinitrobenzene)sulfonamidophenyl]-10,20-diphenylporphyrin (2tSAM). The solid residue was chromatographed [silica, $\text{CH}_2\text{Cl}_2 \rightarrow \text{CH}_2\text{Cl}_2$ /methanol (49:1)], and all fractions containing the product were combined and evaporated to dryness to afford a purple solid 2tSAM.

Alternate Synthesis of 2tSAM. A sample of porphyrin 2t (13 mg, 0.02 mmol)²⁶ was dissolved in anhydrous pyridine (2 mL) followed by addition of 2,4-dinitrobenzenesulfonyl chloride (54 mg, 0.20 mmol). The reaction mixture was subjected to stirring 18 h at room temperature. Upon completion, 1 M HCl (3 mL) was added to the reaction mixture, followed by the addition of CH_2Cl_2 (15 mL). The organic layer was separated, dried over anhydr MgSO_4 , filtered, and evaporated to dryness. The solid residue was chromatographed [silica, $\text{CH}_2\text{Cl}_2 \rightarrow \text{CH}_2\text{Cl}_2$ /methanol (49:1)], and all fractions containing the product were combined and evaporated to dryness to afford a purple solid 2tSAM (18 mg, 81%): UV/vis (DMF) λ_{max} (log ϵ) 421 (4.57), 520 (3.50), 567 (3.45), 657 (3.21) nm; ^1H NMR (500 MHz, DMF- d_7) δ -2.79 (br s, 2H), 7.78 (d, $J = 8.0$ Hz, 4H), 7.88 (d, $J = 6.5$ Hz, 6H), 8.29 (m, 8H), 8.72 (d, $J = 9.0$ Hz, 2H), 8.89 (br m, 10H), 9.13 (d, $J = 2.0$ Hz, 2H), 11.49 (s, 2H) ppm; ^{13}C NMR (125 MHz, DMF- d_7) δ 115.9, 120.5, 121.6, 128.1, 128.4, 133.8, 136.5, 138.2, 142.8, 149.7, 151.8 ppm; ESI-MS obsd 1105; HRMS (ESI+ of $[\text{MH}^+]$, CH_3CN): m/z calcd for $\text{C}_{56}\text{H}_{36}\text{N}_{10}\text{O}_{12}\text{S}_2$ 1105.2028, found 1105.2016; HPLC $t_{\text{R}} = 18.15$ min (using a gradient of 60% to 0% of buffer A over 25 min).

5,0,15-Tris[4-*N*-(2,4-dinitrobenzene)sulfonamidophenyl]-20-phenylporphyrin (3SAM). A solution of porphyrin 3 (23 mg, 35 μmol)²⁶ in anhydrous pyridine (3.0 mL) was treated with

2,4-dinitrobenzenesulfonyl chloride (93 mg, 0.35 mmol). The reaction mixture was stirred at room temperature for 22 h. Upon completion, 1 M HCl (4 mL) was added to the reaction mixture, followed by the addition of CH₂Cl₂ (20 mL) and THF (10 mL). The organic layer was separated, dried over anhydr MgSO₄, filtered, and evaporated to dryness. The solid residue was chromatographed [silica, CH₂Cl₂ → CH₂Cl₂/methanol (49:1)], and all fractions containing the product were combined and evaporated to dryness followed by precipitation from CH₂Cl₂ and hexanes to afford a dark purple solid (37 mg, 78%): UV/vis (DMF) λ_{max} (log ε) 422 (5.42), 570 (5.00) nm; λ_{em} (DMF) 653 nm; ¹H NMR (500 MHz, DMF-*d*₇) δ -2.83 (br s, 2H), 7.77 (d, *J* = 8.5 Hz, 6H), 7.89 (d, *J* = 7.5 Hz, 4H), 8.28 (m, 9H), 8.72 (m, 3H), 8.88 (br m, 10H), 9.13 (br s, 2H), 11.48 (s, 3H) ppm; ¹³C NMR (125 MHz, DMF-*d*₇) δ 119.7, 119.8, 120.8, 120.9, 127.4, 133.0, 134.8, 135.7, 136.8, 137.4, 148.9, 151.0 ppm; ESI-MS obsd 1350; HRMS (ESI+ of [MH⁺], CH₃CN) *m/z* calcd for C₆₂H₃₉N₁₃O₁₈S₃ 1350.1771, found 1350.1752; HPLC *t*_R = 17.36 min (using a gradient of 60% to 0% of buffer A over 25 min).

5,10,15,20-Tetrakis[4-*N*-(2,4-dinitrobenzene)sulfonamido-phenyl]porphyrin (4SAM). A solution of porphyrin **4** (0.13 g, 0.20 μmol)³¹ in pyridine (40 mL) was treated with 2,4-dinitrobenzenesulfonyl chloride (0.43 g, 1.6 mmol). The reaction mixture was stirred at room temperature for 24 h. Upon completion, 1 M HCl (30 mL) was added to the reaction mixture, followed by the addition of CH₂Cl₂ (100 mL) and MeOH (25 mL). The organic layer was separated and concentrated. The solid residue was purified by passing through a pad of silica gradually eluting with CH₂Cl₂, acetone, and acetone/MeOH/TEA (95:4.5:0.5) to afford a dark red solid. The solid residue was dissolved in acetone followed by precipitation with diethyl ether to yield a red solid precipitate (0.16 g, 50%): UV/vis (DMF) λ_{max} (log ε) 440 (5.3) nm, 577 (4.52), 663 (4.18); λ_{em} (DMF) 653 nm; ¹H NMR (500 MHz, DMSO-*d*₆) δ -3.04 (br s, 2H), 7.54 (d, *J* = 8.5 Hz, 8H), 8.13 (d, *J* = 8.0 Hz, 8H), 8.52 (d, *J* = 8.5 Hz, 4H), 8.75 (s, 8H), 8.76 (d, *J* = 2.5 Hz, 2H), 8.78 (d, *J* = 2.0 Hz, 2H), 9.03 (d, *J* = 2.5 Hz, 4H), 11.51 (s, 4H) ppm; ¹³C NMR (125 MHz, DMSO-*d*₆) δ 119.1, 119.8, 120.4, 127.4, 131.9, 135.2, 136.0, 136.4, 138.0, 147.9, 150.2 ppm; ESI-MS obsd 1596.6; HRMS (ESI+ of [MH⁺], CH₃CN) *m/z* calcd for C₆₈H₄₂N₁₆O₂₄S₄ 1595.1513, found 1595.1490; HPLC *t*_R = 16.68 min (using a gradient of 60% to 0% of buffer A over 25 min).

5,10,15-Tris[4-*N*-(PEG)₂amidophenyl]-20-phenylporphyrin (7). A solution of porphyrin **3** (53 mg, 0.08 mmol)²⁶ in CHCl₃/pyridine (5 mL, 4:1) was treated with DCC (0.12 g, 0.60 mmol) and *N*-Fmoc-amido-dPEG2-acid (**5**, 0.21 g, 0.52 mmol). The reaction mixture was subjected to microwave irradiation with the following settings: *T* = 100 °C, *t* = 40 min, power = 300 W, *P*_{max} = off. Upon completion, the reaction mixture was filtered to remove DCU and concentrated. The resulting solid residue was chromatographed [silica, CH₂Cl₂ → CH₂Cl₂/methanol (49:1)], and all fractions containing the product were combined and evaporated to dryness to afford porphyrin **6** as a purple solid (0.14 g, 97%): ESI-MS obsd 1805, calcd 1802.8 (C₁₁₀H₁₀₂N₁₀O₁₅). The title compound was used in the next step without further characterization. A sample of porphyrin **6** (0.14 g, 0.08 mmol)

was treated with DMF/piperidine (20 mL, 3:1). The reaction mixture was stirred at room temperature for 3 h. Upon complete removal of the Fmoc protecting groups the reaction mixture was concentrated. The resulting residue was purified by preparative HPLC (using a gradient of 80% to 20% of buffer A), and all fractions containing the product were combined and evaporated to dryness to afford porphyrin **7** as a dark green solid (66 mg, 73% overall yield in two steps): UV/vis (DMF) λ_{max} (log ε) 424 (4.92), 518 (3.36), 554 (3.35), 596 (2.96), 650 (2.90) nm; λ_{em} (DMF) 660 nm; ¹H NMR (500 MHz, MeOH-*d*₄) δ 2.89 (t, *J* = 6.0 Hz, 6H), 3.17 (t, *J* = 5.0 Hz, 6H), 3.79 (br m, 18H), 4.01 (t, *J* = 6.0 Hz, 6H), 8.04 (br m, 3H), 8.31 (d, *J* = 8.0 Hz, 6H), 8.55 (m, 8H), 8.81 (br m, 8H) ppm; ¹³C NMR (125 MHz, MeOH-*d*₄) δ 38.7, 40.9, 68.1, 68.3, 71.5, 71.6, 120.7, 123.6, 129.6, 130.8, 131.2, 137.3, 138.9, 139.8, 141.5, 142.2, 173.0 ppm; ESI-MS obsd 1136; HRMS (ESI+ of [MH⁺], CH₃CN) *m/z* calcd for C₆₅H₇₂N₁₀O₉ 1137.5557, found 1137.5582; HPLC *t*_R = 7.91 min (using a gradient of 80% to 20% of buffer A over 20 min).

5,10,15-Tris[4-*N*-(2,4-dinitrobenzene)sulfonamido(PEG)₂-amidophenyl]-20-phenylporphyrin (8). A solution of porphyrin **7** (23 mg, 0.02 μmol) in DMF/TEA (5 mL, 9:1) was treated with 2,4-dinitrobenzenesulfonyl chloride (0.11 g, 0.40 mmol). The reaction mixture was stirred at room temperature for 2 days under argon atmosphere. Upon completion, methanol was added to the reaction mixture, followed by the addition of ethyl acetate and water. The organic layer was separated, dried over anhydr MgSO₄, filtered, and evaporated to dryness. The solid residue was chromatographed [silica, CH₂Cl₂/methanol (99:1 → 19:1)], and all fractions containing the product were combined and evaporated to dryness to afford an orange-red solid as a second fraction which was further purified by preparative HPLC (using a gradient of 60 to 0 of buffer A with flow rate 21 mL/min; buffer A = 100:0.1 water/TFA, buffer B = 90:10:0.1 CH₃CN/water/TFA), and all fractions containing the product were combined and evaporated to dryness to afford a light green solid (5 mg, 14%): UV/vis (DMF) λ_{max} (log ε) 422 (5.15), 518 (3.75), 554 (3.63), 594 (3.26), 650 (3.30) nm; λ_{em} (DMF) 656 nm; ¹H NMR (500 MHz, DMF-*d*₇) δ -2.75 (br s, 2H), 2.84 (t, *J* = 6.0 Hz, 6H), 3.39 (m, 6H), 3.61 (br m, 18H), 3.91 (t, *J* = 6.0 Hz, 6H), 7.90 (m, 3H), 8.23 (br m, 11H), 8.33 (m, 2H), 8.50 (br m, 6H), 8.75 (m, 3H), 8.95 (br m, 9H), 10.49 (s, 3H) ppm; ¹³C NMR (125 MHz, DMF-*d*₇) δ 38.0, 43.7, 67.3, 69.7, 70.2, 70.3, 117.8, 120.5, 127.6, 132.3, 135.3, 139.3, 140.1, 148.4, 150.3, 170.2 ppm; ESI-MS obsd 1826; HRMS (ESI+ of [MH⁺], CH₃CN) *m/z* calcd for C₈₃H₇₈N₁₆O₂₇S₃ 1827.4457, found 1828.4423; HPLC *t*_R = 13.76 min (using a gradient of 60% to 0% of buffer A over 25 min).

Acknowledgment. We thank Dr. Scott A. Hilderbrand for his helpful discussions. This work was supported in part by NIH grants U24-CA092782 (RW), U01-HL080731 (JM, RW), U54-CA119349 (RW), and U54-CA126515 (RW). NMR data were obtained at the Department of Chemistry, University of Connecticut, with great thanks to Dr. Martha Morton.

Supporting Information Available: General synthetic and photophysical characterization procedures, fluorescence activation of tertiary SPP with thiols, synthetic procedures for tertiary SPP, NMR (¹H and ¹³C) of all compounds synthesized and HPLC traces of relevant compounds. This material is available free of charge via the Internet at <http://pubs.acs.org>.

(31) Yuasa, M.; Oyaizu, K.; Yamaguchi, A.; Kuwakado, M. *J. Am. Chem. Soc.* **2004**, *126*, 11128–11129.